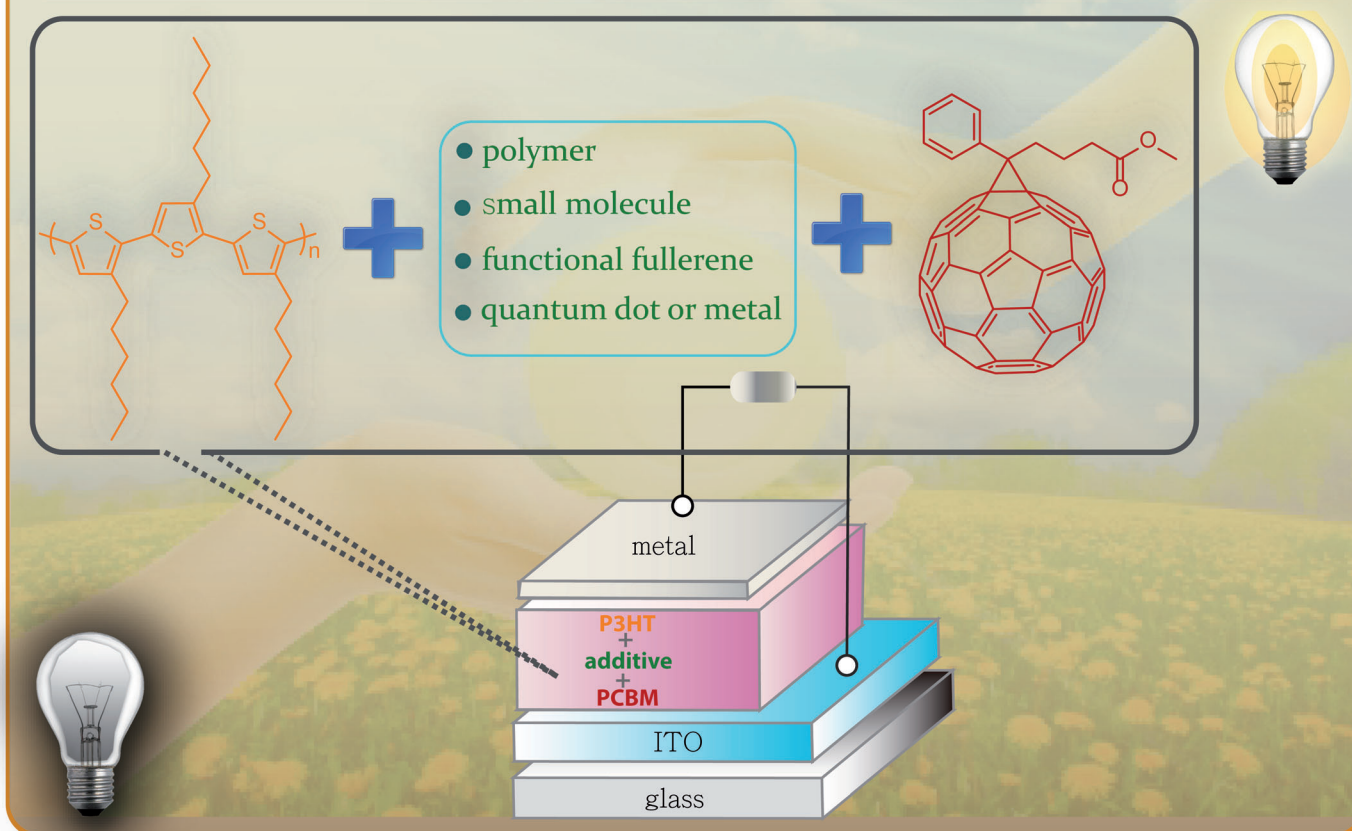
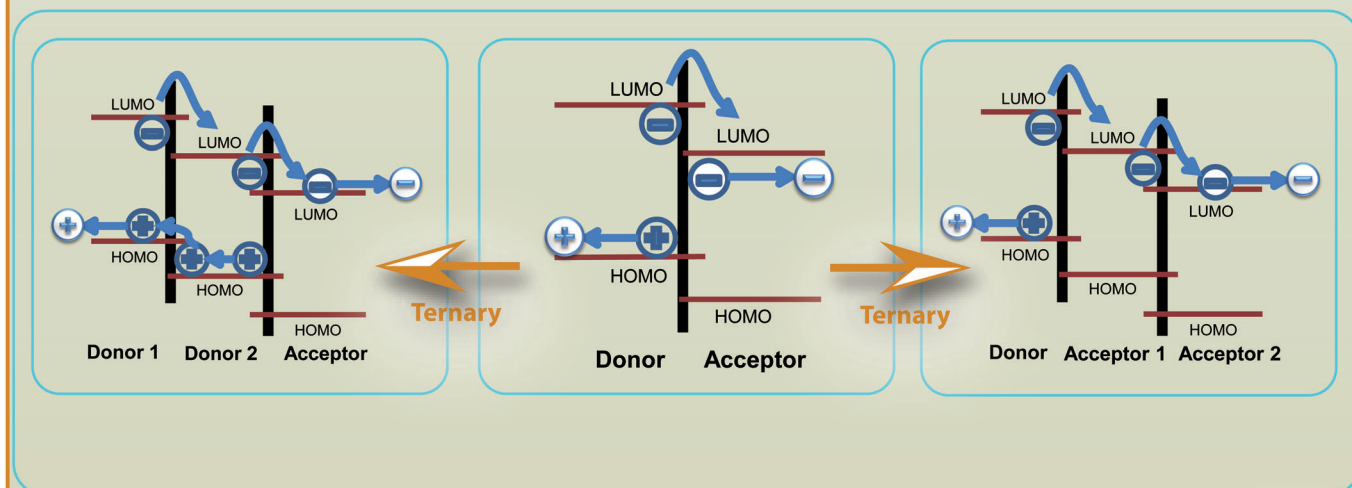


DOI: 10.1002/cssc.201200609

Materials for the Active Layer of Organic Photovoltaics: Ternary Solar Cell Approach

Yung-Chung Chen,^[a] Chih-Yu Hsu,^[a] Ryan Yeh-Yung Lin,^[a, b] Kuo-Chuan Ho,^[b] and Jiann T. Lin^{*[a]}

Ternary for Better Performance



Power conversion efficiencies in excess of 7% have been achieved with bulk heterojunction (BHJ)-type organic solar cells using two components: p- and n-doped materials. The energy level and absorption profile of the active layer can be tuned by introduction of an additional component. Careful design of the additional component is required to achieve optimal panchromatic absorption, suitable energy-level offset, balanced

electron and hole mobility, and good light-harvesting efficiency. This article reviews the recent progress on ternary organic photovoltaic systems, including polymer/small molecule/functional fullerene, polymer/polymer/functional fullerene, small molecule/small molecule/functional fullerene, polymer/functional fullerene I/functional fullerene II, and polymer/quantum dot or metal/functional fullerene systems.

1. Introduction

The increasing rate of fossil-fuel consumption, its accompanying greenhouse effect, and other negative environmental impacts have resulted in research efforts that focus on renewable energy technologies. Among these, organic photovoltaic cells (OPVs) allow for device fabrication of large areas of lightweight and flexible substrates using low-cost solution-processing methods.^[1–4] OPVs are normally comprised of p-doped (electron donor) and n-doped (electron acceptor) materials that are combined to form an active layer, the so-called bulk heterojunction (BHJ). Figure 1 provides a diagram of the architecture

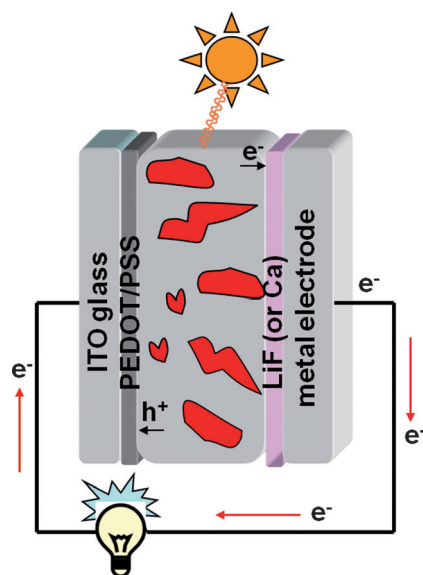


Figure 1. Architecture of an OPV cell.

of a typical BHJ solar cell. The cell is composed of five components: i) a support substrate coated with a transparent conduc-

tive oxide (indium tin oxide, ITO); ii) a thin layer of poly(3,4-ethylenedioxythiophene):poly(styrenesulfonate) (PEDOT:PSS) as hole injection layer; iii) an active layer comprising p- and n-doped materials; iv) a thin buffer layer, such as Ca or LiF, for adjusting the energy level; and v) a metal electrode, such as Al, as the cathode.

Under light illumination, the light-absorbing dye (normally the donor component) is excited, and an electron–hole pair forms. The electron–hole pair (the localized exciton) then diffuses to the donor–acceptor (D–A) interface, where it is transformed into a charge-transfer exciton, D^+A^- . Subsequent charge separation results in the formation of D^+ (hole) and A^- (electron) polarons. Finally, the electron migrates to the cathode and the hole migrates to the anode to complete the OPV electricity generation cycle. Recombination of D^+ and A^- may occur during transport, which reduces the charge-collection efficiency. An OPV cell's recombination rate is suppressed more effectively using a BHJ configuration than it is for an n–p layer arrangement because the distance between the absorption site and the D–A interface is shorter in the BHJ cell.^[5] Power conversion efficiencies in excess of 7% are obtainable for OPVs based on polymers or small molecules with fullerene derivatives.^[6] Design rules for the selection of donor materials for the optimization of BHJ-cell efficiency include using materials with a low highest occupied molecular orbital (HOMO) energy level to achieve a higher open-circuit voltage (V_{oc}), a low band gap for good light harvesting, appropriate crystallinity and morphology to provide high carrier mobility, and well-matched HOMO and lowest unoccupied molecular orbital (LUMO) energy levels between the donor and the acceptor materials for efficient charge separation.^[2,5,7]

To realize the commercialization of low-cost OPVs, improvements in cell performance, materials design, and device-manufacturing methods are required. Ideally, a cell would harvest all photons with a wavelength less than approximately 920 nm for conversion into an electric current.^[8] To provide a broader absorption profile, a simple approach to increasing the photon flux density is to use a mixture of sensitizers that absorb in different wavelength regions. This approach was realized in inorganic thin-film solar cells over several decades, and also attempts have been made to implement this approach in OPVs.^[9] In this Review, we focus our discussion on the recent developments, especially on those accomplished in the last five years, in ternary organic solar cells that offer improvements in OPV light harvesting over the entire visible and near-infrared (NIR) spectrum. This Review systematically discusses OPV systems of various configurations, such as organic materi-

[a] Dr. Y.-C. Chen, Dr. C.-Y. Hsu, R. Y.-Y. Lin, Prof. J. T. Lin
Institute of Chemistry
Academia Sinica
128 Academia Road Sec. 2, Nankang Taipei, 115 Taiwan (ROC)
Fax: (+886) 2-27831237
E-mail: jtlin@gate.sinica.edu.tw

[b] R. Y.-Y. Lin, Prof. K.-C. Ho
Department of Chemical Engineering
National Taiwan University
No. 1, Sec. 4, Roosevelt Road, Taipei, 106 Taiwan (ROC)

al/organic material/functional fullerene, organic material/functional fullerene I/functional fullerene II, and organic material/quantum dot or metal/functional fullerene systems.

2. Fundamental Design of Ternary Solar Cells

Ideally, all photons with a wavelength below roughly 920 nm that fall on an OPV should be harvested and converted into an electric current.^[8] In addition to complementary absorption, several criteria must be met for mixtures of sensitizers to provide good cell performance in a ternary OPV device, such as

Dr. Yung-Chung Chen received his PhD degree in Chemical Engineering in 2009 from the National Chung Hsing University, Taiwan, under the supervision of Professor Ru-Jong Jeng. Afterwards, he joined Prof. Jiann T. Lin's group as a postdoctoral fellow at the Institute of Chemistry, Academia Sinica, Taiwan. His current research interest is focused on the synthesis and characterization of organic and polymeric functional materials for optoelectronic and photovoltaic applications, and the fabrication of solar cells and OLED (organic light-emitting diode) devices.



Dr. Chih-Yu Hsu received his B.Sc. degree from the Department of Chemical Engineering at the National Taiwan University, Taiwan, in 2005. He received his Ph.D. in Chemical Engineering from the same university in 2010 under the supervision of Prof. Kuo-Chuan Ho. Currently he is a postdoctoral fellow in Prof. Jiann T. Lin's laboratory at the Institute of Chemistry, Academia Sinica, Taiwan. His research interests cover electrochemical analysis based on chemically modified electrodes and applications of electrochemistry to electro-optical devices.



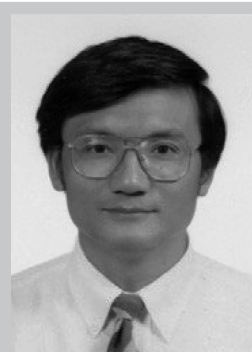
Ryan Yeh-Yung Lin received his master degree from the Department of Chemical Engineering at the National Taiwan University of Science and Technology (2010). He is now a Ph.D. student at the Department of Chemical Engineering, National Taiwan University, Taiwan. He performs research in conjunction with Prof. Kuo-Chuan Ho and Prof. Jiann T. Lin's laboratory. His research focuses on the synthesis of organic dyes, ion-liquid electrolytes, and their application to photoelectrochemical devices.



a suitable offset of the various blended components' energy levels and balanced carrier mobility between electron acceptor (electron transport) and electron donor (hole transport).

Two prototypical energy profiles of ternary systems are shown in Figure 2. The HOMO and LUMO energy levels of the ternary systems are important parameters for determining the cell performance. In these "two donor/one acceptor" (Figure 2a) and "one donor/two acceptor" (Figure 2b) systems, the cascade energy levels must have the correct offset with respect to those of their doped counterparts. In principle, the addition of a third component to a binary system could affect the film morphology. Thus, it is important to control the ratios of components in the active layer. Recently, a new type of cell with two donors and one acceptor was reported. In this BHJ solar cell, there is no need for an energy cascade between the two donors. In contrast to the systems in Figure 2, V_{oc} in this system is not pinned to the lower V_{oc} value of the two binary donor/acceptor cells. However, the detailed working mechanism remains to be further investigated (*vide infra*).

Dr. Kuo-Chuan Ho received his B.Sc. and M.Sc. degrees from the Department of Chemical Engineering at the National Cheng Kung University, Taiwan, in 1978 and 1980, respectively. He received his Ph.D. in Chemical Engineering from the University of Rochester, USA, in 1986. Currently he is a Distinguished Professor jointly appointed by the Department of Chemical Engineering and the Institute of Polymer Science and Engineering at the National Taiwan University, Taiwan. His research interests mainly surround applications of chemically modified electrodes on sensing and electro-optical devices, including dye-sensitized solar cells and electrochromic devices.



Prof. Jiann T. Lin received his B.Sc. degree in Chemistry from the National Tsing Hua University, Taiwan, in 1975. He completed his PhD in the Chemistry Department of the University of Minnesota, USA, in 1984. After a year as postdoctoral fellow in the Chemistry Department of the University of Michigan, USA, he joined the Institute of Chemistry, Academia Sinica, Taiwan, as an Associate Research Fellow in 1984, and was promoted to Research Fellow in 1990. He was a visiting scholar in the Northwestern University, USA, in 1991. Dr. Lin is also Adjunct Professor of the National Central University, Taiwan. His current scientific interests involve the studies of organic materials for organic light-emitting diodes, organic solar cells, and two-photon absorption dyes.



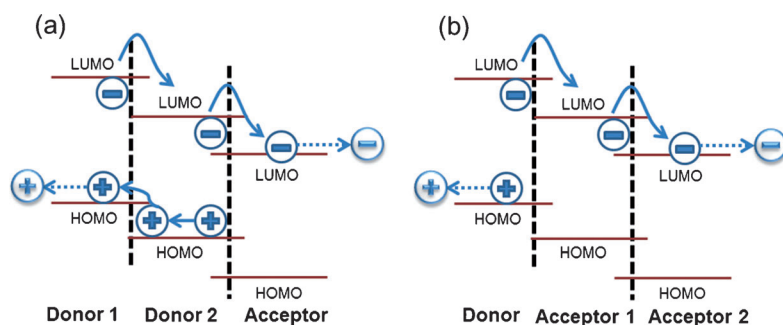


Figure 2. Ternary system energy diagrams.

3. Molecular Design of Ternary Solar Cells

3.1. Polymer/small molecule/PCBM-based ternary solar cells

Poly(3-hexylthiophene) (P3HT) is the most commonly used p-doped material; BHJ solar cells based on P3HT and [6,6]-phenyl- C_{61} butyric acid methyl ester (PCBM) achieve up to 5% solar power conversion efficiency.^[1,10,11] However, P3HT only absorbs approximately 25% of incident light, and thus limits the maximum available photocurrent density.^[12] Researchers have attempted to dope P3HT by using small molecules with complementary absorption characteristics, for example, by doping high-efficiency light-harvesting polymers with p-doped materials to form a ternary component. In this section, we discuss small molecules including metal complexes and metal-free compounds that are used as doping additives.

3.1.1. Metal complexes

In 2009, Ohkita et al. reported the synthesis of NIR-absorbing Zn-based (ZnPc) and silicon-based (SiPc) phthalocyanine dyes (Figure 3).^[13] These dye molecules were used as the ternary component of the P3HT/PCBM active layer and provide improvements in light-harvesting efficiency at longer wavelengths, extending into the NIR region.

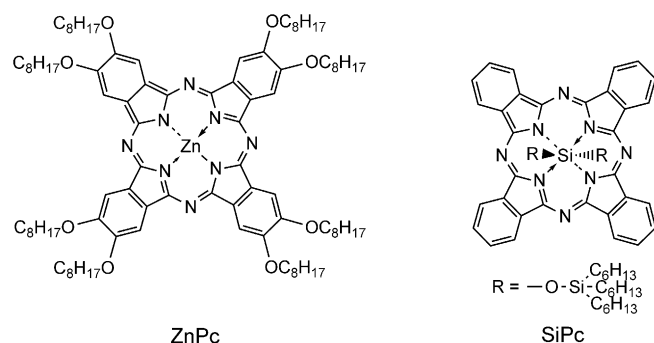


Figure 3. Structures of Zn- (ZnPc) and Si-based (SiPc) phthalocyanine dyes.

After thermal annealing, a device based on the P3HT/PCBM/SiPc 1:1:0.07 (w/w/w) ternary blend produced a photocurrent (J_{sc}) of 7.9 mA cm^{-2} and power conversion efficiency (PCE) of

2.7% improved over those quantities of the pristine P3HT/PCBM (annealed) device (6.5 mA cm^{-2} ; 2.2%).^[13] By contrast, a device based on the P3HT/PCBM/ZnPc ternary blend had a lower PCE (1.1%) than the pristine P3HT/PCBM (annealed) cell; this difference was attributed to the aggregation of dye molecules, which resulted in a lower effective absorption coefficient.^[13] The improved performance of the P3HT/PCBM/SiPc compared

to the P3HT/PCBM device was attributed to the dual functions of SiPc as i) a sensitizer with complementary absorption characteristics and ii) a long-range energy acceptor of P3HT excitons at the D–A interface that facilitate charge separation. Energetic cascades in both the HOMO and LUMO energy levels at the interface facilitate SiPc exciton electron injection into PCBM and hole injection into P3HT.

Ohkita et al. applied transient absorption spectroscopy to the P3HT/PCBM/SiPc ternary system for a more detailed mechanistic insight.^[14] After excitation of the thermally annealed blend films, a fast energy transfer from P3HT excitons occurs, which results in the formation of SiPc excitons because of the large spectral overlap between P3HT emission and SiPc absorption wavelengths. Subsequent charge transfer between P3HT and SiPc excitons generates P3HT polarons and SiPc anions; charge transfer from the SiPc anions to PCBM then readily occurs. Ohkita concluded that SiPc molecules were inhomogeneously distributed at the P3HT/PCBM interface with close contact with both P3HT and PCBM. Consequently, light harvesting, based on both dye sensitization and polymer exciton collection, is highly efficient in ternary blend solar cells.

Later, the same group developed quaternary OPVs using two NIR sensitizers, SiNc (Figure 4) and SiPc (Figure 3), as the additives.^[15] SiNc exhibits spectral absorption at longer wavelengths than SiPc and has a better energy level alignment with P3HT and PCBM.

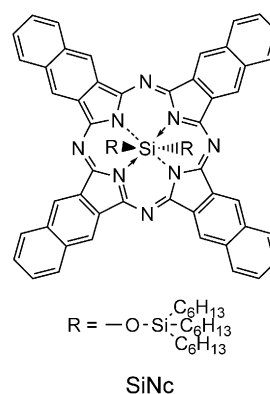


Figure 4. Structure of the SiNc-based phthalocyanine dye.

The UV/Vis absorption spectra of the blended materials and the external quantum efficiency (EQE) spectra of their OPVs are shown in Figure 5. Two absorption bands at roughly 670 and

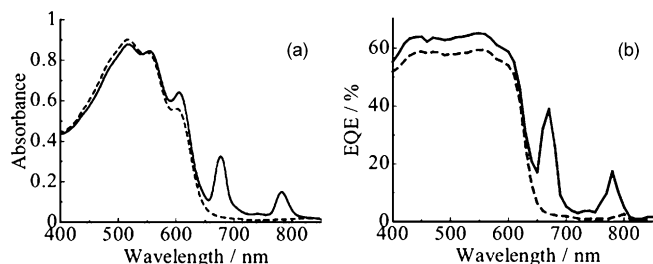


Figure 5. (a) Absorption spectra of the P3HT/PCBM/SiPc composite (4.8 wt%)/SiNc (1.5 wt%) blend (solid line) and P3HT/PCBM blend film (broken line). (b) EQE spectra of the ITO/PEDOT:PSS/P3HT/PCBM/SiPc/SiNc/Ca/Al (solid lines) and the ITO/PEDOT:PSS/P3HT/PCBM/Ca/Al device (broken lines). Reprinted with permission from Ref.[15]. Copyright 2010, The Royal Society of Chemistry.

780 nm were assigned to SiPc and SiNc, respectively. Furthermore, P3HT/PCBM showed a broad absorption at 400–600 nm. P3HT crystallization was not disturbed by the addition of the additional dye, as evidenced by an absorption band at 600 nm. Two sharp peaks at 670 and 780 nm in the EQE spectra clearly indicate the two dyes' contributions to the photocurrent. The P3HT/PCBM/SiPc/SiNc quaternary blend solar cell exhibited a higher PCE (4.3%) than the individual ternary blend solar cells of P3HT/PCBM/SiPc (4.1%), P3HT/PCBM/SiNc (3.7%), or the pristine cell of P3HT/PCBM (3.5%); the authors attributed this superior performance to the broad light-harvesting range, up to 800 nm, of the quaternary blend solar cell.^[15]

BODIPY (4,4-difluoro-4-bora-3a,4a-diaza-s-indacene) derivatives possess both chemical and photostability and also exhibit long-wavelength absorption suitable for solar cell applications.^[16] NIR-absorbing BODIPY dyes **1a** and **1b** (Figure 6) were investigated by Kubo et al. and used in ternary OPVs for the first time.^[17] These NIR dyes (**1a**, $\lambda_{\text{max}}=733$ nm; **1b**, $\lambda_{\text{max}}=747$ nm) are beneficial for the long-wavelength absorption, and enhance the BHJ solar cell light-harvesting capacity. After blending 5 wt% of **1a** or **1b** into the active layer of P3HT/IC₇₀BA, PCE increased from 3.7 to 4.3 and 4.0% for **1a** and **1b**, respectively. The authors attributed the high J_{sc} and PCE values to improvements in NIR light harvesting.

Porphyrin-based materials have high optical absorption characteristics in the visible spectrum and high hole mobility,^[18,19] they are suitable for OPV applications. Dastoor et al. used a porphyrin-based dye, (Cu(CN)₄PP), with a Soret band at 445 nm and Q band at 635 nm (Figure 7), as the third component in the active layer of P3HT:PCBM devices.^[20] Although the UV/Vis spectra showed a porphyrin contribution, the performances of the ternary porphyrin-blended OPV devices were substantially inferior to those of the binary devices without the porphyrin dye. After annealing, the dye-generated photocurrent was lost, except in devices where only a small amount of poly-

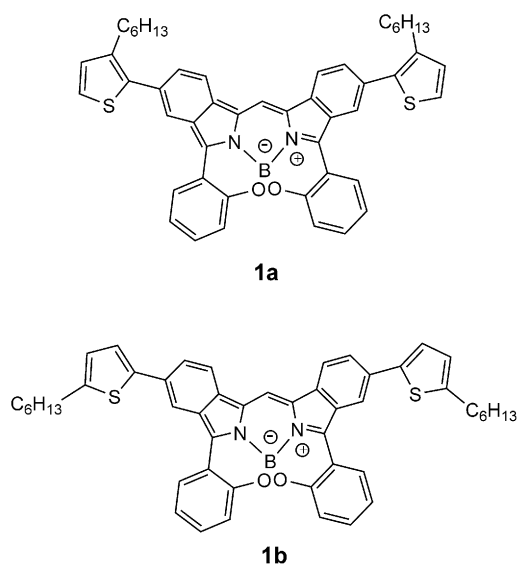


Figure 6. Structures of BODIPY dyes (**1a**, **1b**).

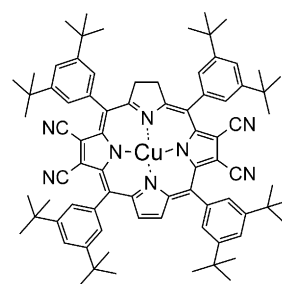


Figure 7. Structure of the porphyrin-based dye (Cu(CN)₄PP).

mer was present. The observed reduction in absorption efficiency and charge mobility of the active layer was attributed to annealing-induced aggregation of porphyrin molecules.

Belcher et al. synthesized three porphyrins, varying only in the steric bulk of their peripheral groups, *p*TP, XyP, and *t*BuPP (Figure 8) and integrated these into the active layers of MEH-PPV/PCBM-based OPVs (MEH-PPV = poly[2-methoxy-5-(20-ethylhexyloxy)-1,4-phenylene-vinylene]).^[21] All the devices exhibited substantially lower efficiencies than the pristine binary system. The addition of porphyrin materials into binary-blend devices affects the electronic structure, rather than the morphology, of the active layer. The porphyrins were thought to

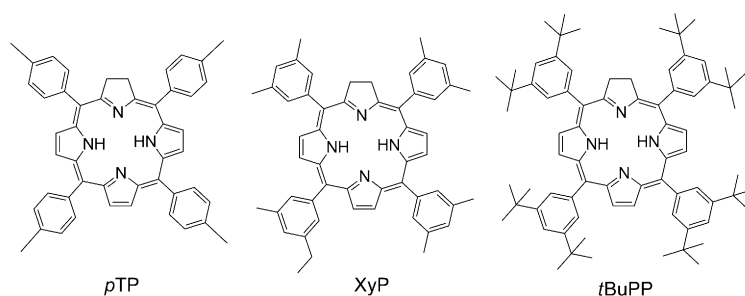


Figure 8. Structures of porphyrins dyes (*p*TP, XyP, *t*BuPP).

act as bound electron-hole pair centers of recombination; the higher efficiency and V_{oc} of the bulkiest porphyrin, *t*BuPP, were accounted for by the increased spatial separation of the bulkier porphyrin molecules, which reduced the charge recombination rate.

In 2011, Roy et al. developed a new dye with NIR absorption characteristics. The copper(II) phthalocyanine dye, CuMePc (Figure 9), exhibited a broad absorption from 600 to 700 nm.^[22]

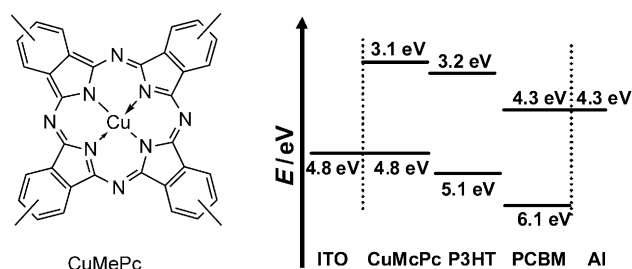


Figure 9. Structure of the copper(II) phthalocyanine dye (CuMePc, left), and the OPV materials' energy level diagram (right).

The ternary OPV, with a P3HT/CuMePc/PCBM ratio of 1:1:2 (*w/w*), exhibited a PCE significantly improved over that of the binary P3HT/PCBM composite OPV (5.3 vs. 3.2%). This enhancement was credited to improved hole mobility and light harvesting. However, the ternary system had a lower V_{oc} than the binary system (0.58 vs. 0.61 V) because of a smaller energy offset between the donor's HOMO and the acceptor's LUMO (Figure 9).

Fujii et al. developed a non-peripheral octahexylphthalocyanine dye, C6PcH₂ (Figure 10), with characteristic NIR absorption and high hole mobility ($1.4 \text{ cm}^2 \text{ V}^{-1} \text{ s}^{-1}$) and good electron mobility ($0.5 \text{ cm}^2 \text{ V}^{-1} \text{ s}^{-1}$).^[23] The compound was used as a dopant in the P3HT/PCBM binary system. The cell with the best performance had an active layer with a P3HT/C6PcH₂/PCBM ratio of 10:3:10; the J_{sc} and cell performance (12.1 mA cm^{-2} ; 3.0%, respectively) were improved compared to the binary cell (8.6 mA cm^{-2} ; 2.3%). Mutual microphase separation occurred in the active layer, of which an XRD study showed the microphase to be comprised of both, highly ordered P3HT domains and hexagonal columnar structures of C6PcH₂.

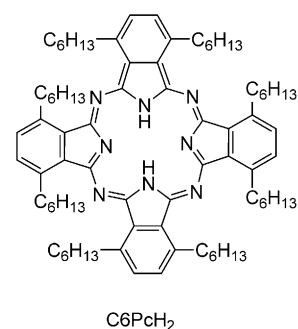


Figure 10. Structure of non-peripheral octahexylphthalocyanine dye (C6PcH₂).

3.1.2. Metal-free compounds

Our group developed a dibenzo[*f,h*]thieno[3,4-*b*]quinoxaline-based dye, TQTFA, for the ternary system, TQTFA/P3HT/PC₇₁BM [PC₇₁BM = ([6,6]-phenyl C₇₁ butyric acid methyl ester), Figure 11].^[24] The matched energy levels of TQTFA, PC₇₁BM, and P3HT allow photogenerated excitons to dissociate into electrons and holes, which are then driven toward the cathode and anode, respectively. Therefore, both the broader absorption profile and energetic cascade between components result in improved J_{sc} and V_{oc} . The best performing device exhibited a power conversion efficiency of 4.50%. The efficiency was increased by almost 15% compared to the device without TQTFA.

Low-band-gap polymers based on 1,4-diketo-3,6-dithienylpyrrolo[3,4-*c*]pyrrole (DPP) have attracted considerable interest in the field of solar cells because of their useful optical properties and their mechanical and thermal stabilities.^[25–27] A small HOMO/LUMO energy gap makes DPP a good candidate for ternary solar cell applications. In 2008, Nguyen et al. developed a small band gap compound, SMD1, based on the DPP core (Figure 12) and incorporated it as the third component in a P3HT/PC₇₁BM BHJ solar cell.^[28]

Absorption spectra of SMD1, P3HT, and PC₇₁BM in the film state are shown in Figure 13. The three components show complementary absorptions and thus are ideal for ternary solar cell applications. Increasing the SMD1 content in the P3HT/PC₇₁BM active layer resulted in increased absorption in the 650–800 nm region. However, the efficiency of the annealed

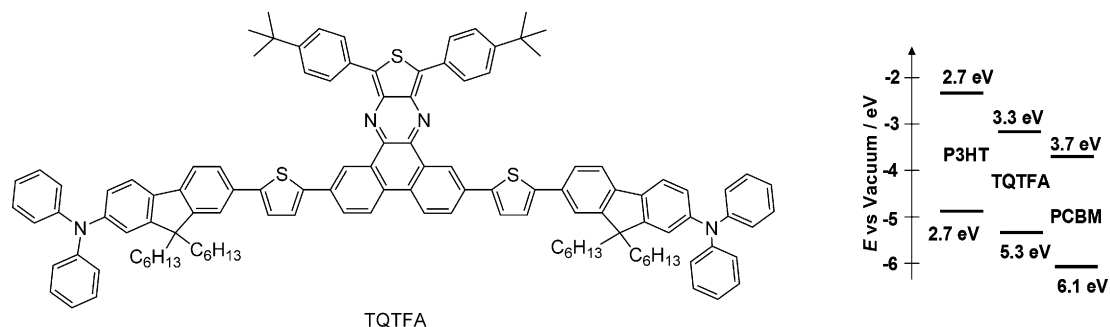


Figure 11. Structure of TQTFA, and the OPV energy level diagram.

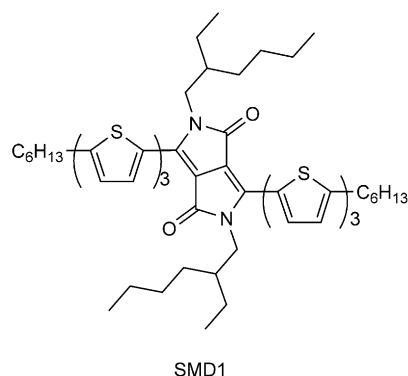


Figure 12. Structure of SMD1.

cell decreased with increasing SMD1 content. The decreased efficiency correlated with a rougher active layer surface. Cells fabricated from solutions containing SMD1 (2 mg mL^{-1}), P3HT (10 mg mL^{-1}), and PC₇₁BM (10 mg mL^{-1}) were annealed for 30 s at 130°C before producing their maximum power conversion efficiency ($J_{\text{sc}} = 8.6 \text{ mA cm}^{-2}$; $V_{\text{oc}} = 0.63 \text{ V}$; $\eta = 3.21\%$).

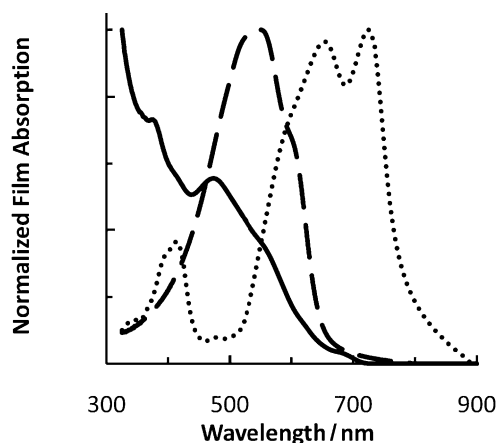


Figure 13. Normalized absorption spectra for thin films of PC₇₁BM (solid), P3HT (dashed), and SMD1 (dotted). Reprinted with permission from Ref. [28]. Copyright 2008, American Institute of Physics.

Yang et al. used DMPA-DTDPP (Figure 14), a DPP-based compound, as an additive for the P3HT/PCBM BHJ solar cell.^[29] The device incorporating 5 wt% DMPA-DTDPP exhibited the highest efficiency at 3.37%, representing an approximate 12% increase relative to the reference cell without additives. This improvement may have resulted from the ternary cell's more efficient light harvesting and reduced surface roughness characteristics compared to the P3HT/PCBM binary cell.

Sharma et al. also reported a new low-band-gap small molecule DPP-CN (Figure 15), a NIR absorber, as an additive for the

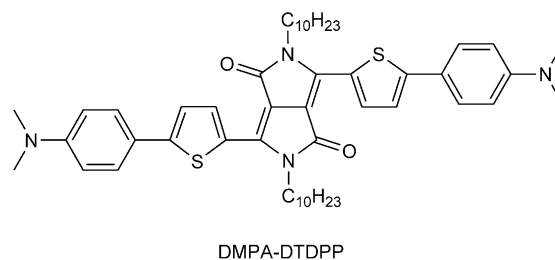


Figure 14. Structure of DMPA-DTDPP.

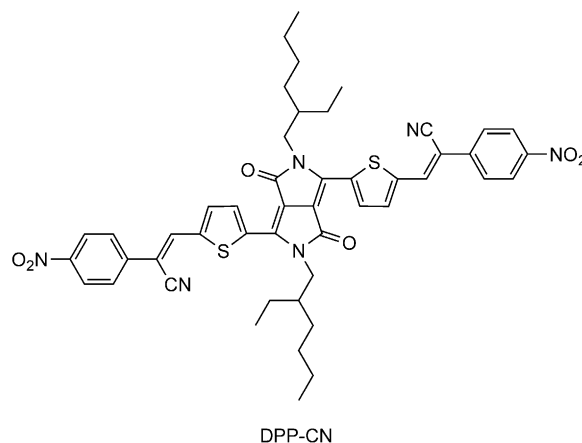


Figure 15. Structure of DPP-CN.

P3HT/PC₇₁BM BHJ solar cell.^[30] The light harvesting property and cascade energy levels resulted in an improved PCE. After optimization, the highest efficiency of 4.7% was achieved with the device incorporating 10 wt% DPP-CN, which was higher than the reference cell without additives ($\eta = 3.23\%$).

Sharma et al. reported the use of a low-band-gap material, BTD-TNP (λ_{abs} in a thin film = 650 nm) as the additive in copolymer P (λ_{abs} in a thin film = 534 nm)/PCBM system (Figure 16).^[31] The P/PCBM/BTD-TNP ternary system, with a 1:1:1 (w/w/w) composite ratio, provided a J_{sc} of 5.8 mA cm^{-2} , a V_{oc} of 0.81 V, and an overall efficiency of 2.6%. The cell efficiency ($\eta = 1.27\%$) was twice that of the annealed P/PCBM copolymer (1:1, w/w) system. Furthermore, thermal annealing improved the device efficiency, indicating that the excitons dissociated more effectively into charge carriers in the presence of BTD-TNP. The incident photon-to-current efficiency (IPCE) spectrum of the

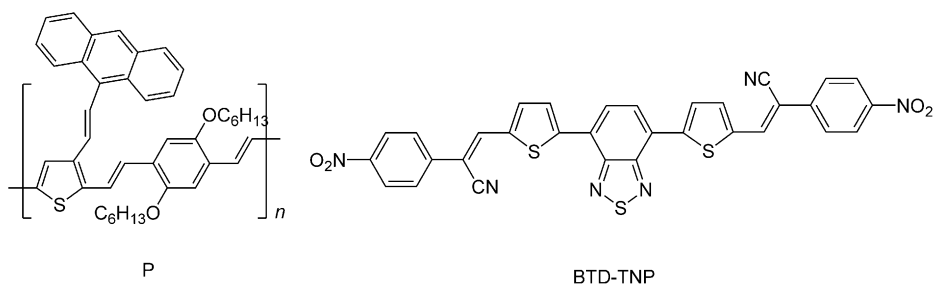


Figure 16. Structures of copolymer P and BTD-TNP.

device in their study shows two strong bands originating from copolymer P and BTD-TNP, indicating the contribution of both copolymer P and BTD-TNP to light harvesting. The authors concluded that BTD-TNP acts as a photosensitizer and also facilitates efficient charge separation by providing a path for copolymer P excitons to migrate toward the P:PCBM interface.

The same authors also developed the low-band-gap compound Se-SM and a new phenylenevinylene copolymer, P2, for use in ternary BHJ systems (Figure 17).^[32] The Se-SM film showed a broad absorption band with λ_{max} at 640 nm. By comparison, λ_{max} for the absorption band of copolymer P2 is roughly 426 nm. Although binary photovoltaic devices operate at low efficiencies (copolymer P2/PCBM = 0.52%, Se-SM/PCBM = 1.30%), the ternary devices showed significant improvement. For example, after thermal annealing, the overall efficiency of P2/Se-SM/PCBM (1:0.5:1 w/w/w) was approximately 3.16%. Again, this performance enhancement arises from increased light harvesting and more effective charge separation.

SM is a sensitizer comprising a thienothiadiazole core and two peripheral cyanovinylene 4-nitrophenyl units (Figure 18); it was used as the third component in a P3HT/PCBM cell.^[33] Incorporation of SM resulted in increases in J_{sc} and V_{oc} and thus the overall efficiency increased to approximately 3.69% compared to the efficiency of the pristine cell (2.9%). Thermal an-

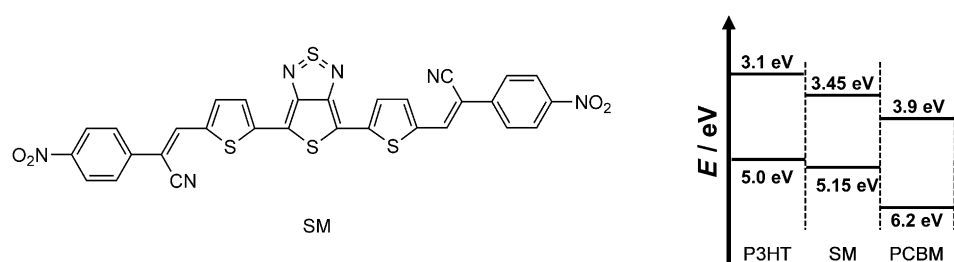


Figure 18. Structure of SM and the OPV energy level diagram.

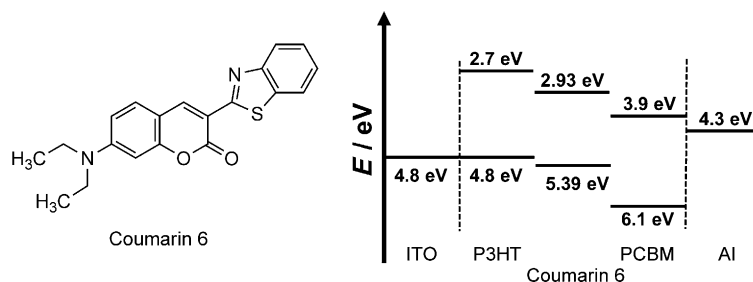


Figure 19. Structure of Coumarin 6 and its energy level diagram.

in 2010 as the third component in a P3HT/PCBM BHJ solar cell.^[34] The dye exhibits good light-harvesting properties at wavelengths comparable to those of P3HT and an energy cascade that is compatible with P3HT and PCBM for both LUMO and HOMO energy levels.^[34] However, both the photocurrent and cell efficiency decrease with increasing Coumarin 6 content. The authors attributed this outcome to the inability of Coumarin 6 to convey excitons and charge carriers through the ternary composite.

Kwon et al. reported the use of HMBI (Figure 20), comprised of electron-donating carbazole and electron-accepting diketone moieties, as the additive for solution-processed BHJ organic solar cells.^[35] P3HT has a broad absorption band between 400 and 550 nm, whereas HMBI absorbs at shorter wavelengths, between 350 and 400 nm (Figure 20). The best performing cell consisted of 3 wt% HMBI dopant and produced the best efficiency of 2.9%, surpassing that of the pristine P3HT/PCBM device at 2.6%. In addition to broadening the OPV device's absorption spectrum, energy transfer from HMBI to P3HT provided more effective charge separation at the P3HT/PCBM interface. An optimized P3HT/HMBI ratio is important for charge transport. At high HMBI concentrations, a large number of dispersed HMBI molecules hinder charge transport, resulting in deteriorated cell performance, as evidenced from AFM images.^[35]

3.2. Polymer/polymer/PCBM-based ternary solar cells

Compared to the additives based on small molecules, polymeric types generally have broader absorption profiles and better atmospheric stability.^[36] Hayashi et al. investigated the effect of the MEH-PPV on the performance of the P3HT/PCBM BHJ solar

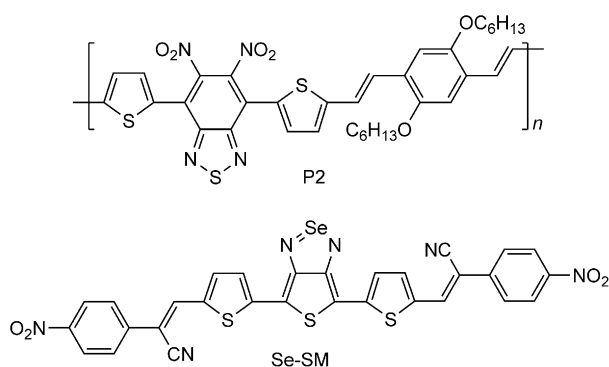


Figure 17. Structures of copolymer P2 and Se-SM.

nealing provided further increases in efficiency, to 4.1%. These gains were attributed to a broader absorption spectrum, which produced increased J_{sc} values, and to greater resolution of energy levels, which yielded the increased V_{oc} values (Figure 18).

There have been attempts to develop additives with wider HOMO/LUMO band gaps. The Coumarin 6 dye (Figure 19) possesses a larger band gap than P3HT; it was used by Ismail et al.

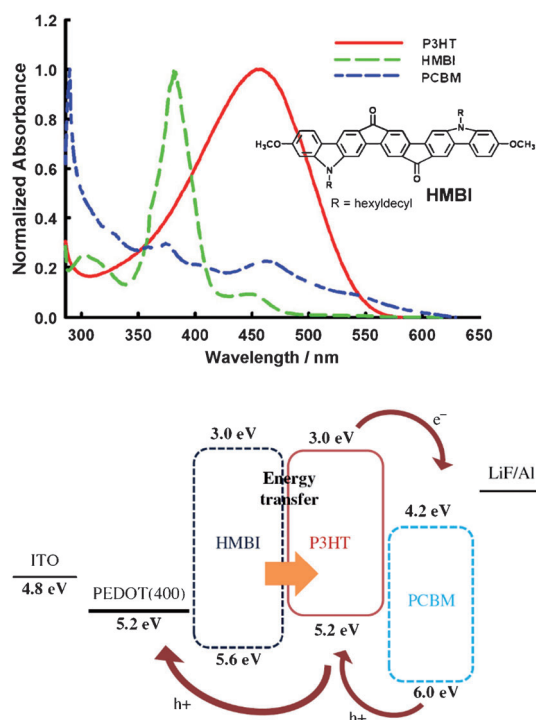


Figure 20. Structure of HMBI and UV/Vis absorption spectra of P3HT, PCBM, and HMBI (top) and the associated energy level diagram (bottom). Reprinted with permission from Ref. [35]. Copyright 2011, Elsevier.

cell.^[37] Introducing MEH-PPV into the active layer yielded an increase in V_{oc} from 0.38 to 0.50 V. This might have resulted from a reduction in the HOMO energy level after introduction of the MEH-PPV polymer. The best power conversion efficiency under 1.5 AM simulated solar illumination (100 mW cm^{-2}) was 1.12%, slightly better than that of the pristine cell (0.85%).

Tai et al. synthesized a new ambipolar polymer poly[2,3-bis-(thiophen-2-yl)-acrylonitrile-9,90-dioctyl-fluorene] (FLC8, shown in Figure 21), with HOMO (−5.68 eV) and LUMO (−3.55 eV) energy levels lying between those of PCBM and P3HT, respectively.^[38] The ambipolar polymer facilitated polaron transport with comparable hole and electron mobility (approx. $10^{-4} \text{ cm}^2 \text{ V}^{-1} \text{ s}^{-1}$). After preparation of the ternary P3HT/PCBM/FLC8 composite (1:0.8:0.05 by weight), the PCE of the ternary solar cell ($\eta = 2.93\%$) increased by approximately 30% compared to the reference cell without FLC8 ($\eta = 2.26\%$). The observed PCE enhancement resulted from improvements in both J_{sc} and FF . The increased J_{sc} was attributed to the more effective charge separation at the donor/acceptor (P3HT/FLC8 and

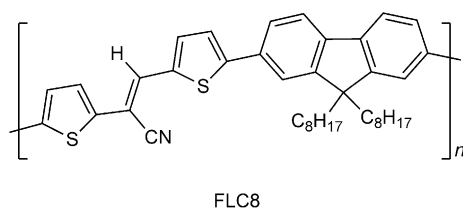


Figure 21. Structure of the FLC8 polymer.

FLC8/PCBM) interfaces because of a favorable energy cascade. By contrast, the improvement in FF resulted from fast charge transfer arising from FLC8s ambipolarity. Reductions in charge recombination resulted in an increased shunt resistance (R_{sh}).

Egbe et al. developed two poly(*p*-phenylene ethynylene)-alt-poly(*p*-phenylene vinylene)-based conjugated polymers, DO-PThE₁-PPV₂ (D1) and MEH-PThE₁-PPV₂ (D2) (Figure 22) with the

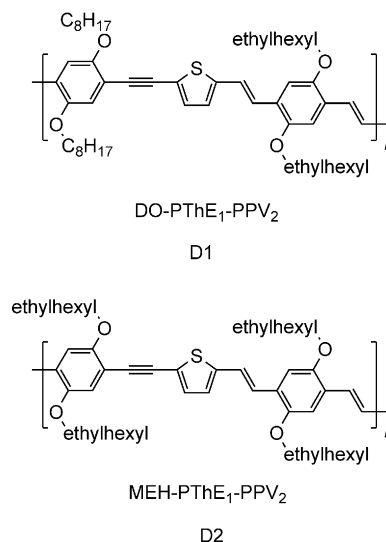
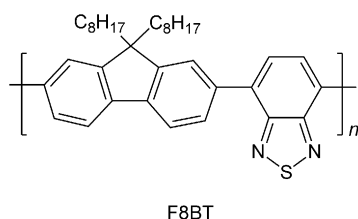


Figure 22. Structures of the DO-PThE₁-PPV₂ (D1) and MEH-PThE₁-PPV₂ (D2) copolymers.

same conjugated backbone but with different types and volume fractions of alkoxy side chains.^[39] Ternary OPVs with a D1/D2/PCBM composite ratio of 0.5:0.5:3 (w/w/w) and binary OPVs with a D1/PCBM or D2/PCBM composite ratio of 1:3 (w/w) were fabricated for comparison. V_{oc} , J_{sc} , and cell efficiency in the ternary system were higher than those of either binary system. AFM images of the three composite films showed that the surface roughness of the ternary system (0.5 nm) was between those of D1 (10.7 nm) and D2 (0.3 nm). The side-chain volume fraction affected the active layer's nanomorphology, and combining D1 and D2 films could be used to optimize the phase separation to improve charge separation. Additionally, hole mobility in the D1–D2 film was $2.6 \times 10^{-4} \text{ cm}^2 \text{ V}^{-1} \text{ s}^{-1}$, which is higher than that of D1 ($1.8 \times 10^{-5} \text{ cm}^2 \text{ V}^{-1} \text{ s}^{-1}$) and D2 ($2 \times 10^{-6} \text{ cm}^2 \text{ V}^{-1} \text{ s}^{-1}$) films, as measured by hole mobility charge extraction using a linearly increasing voltage (CELIV). CELIV results showed that the D1–D2 film formed a new intermolecular arrangement, favorable for a higher charge carrier mobility compared to the individual D1 and D2 polymers. Consequently, the most efficient ternary cell exhibited a PCE of 2.0%.

Electron-deficient benzothiadiazole is often used for the synthesis of polymers that absorb at longer wavelengths.^[40,41] Kim et al. fabricated a ternary system based on a soluble fullerenes and two conjugated polymers, P3HT and the benzothiadiazole compound F8BT (Figure 23), as P3HT/PCBM/F8BT at a ratio of 1:0.6:1.4 (w/w/w) under different thermal annealing conditions.^[42] Cell efficiency was optimized at an annealing tempera-

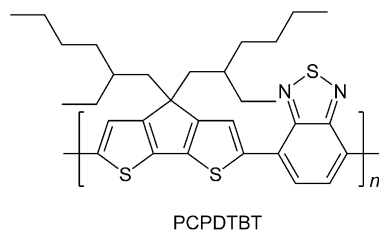


F8BT

Figure 23. Structure of P8BT.

ture of 130 °C. At 1.94%, the efficiency of the P3HT/PCBM/F8BT ternary cell with a composition ratio of 1:0.6:1.4 (w/w/w) was higher than that of the P3HT/PCBM binary system (1.38%) with a composition ratio of 1:2. However, an optimized binary system comprising P3HT/PCBM with a 1:1 ratio operated at 3.16% cell efficiency; it is possible that the low carrier mobility of F8BT resulted in a low cell photocurrent.

Koppe et al. used NIR-absorbing PCPDTBT (Figure 24) as an additive in the P3HT/PCBM system.^[43] This offered two advantages: i) PCPDTBT absorbs well in the NIR region, and ii) the



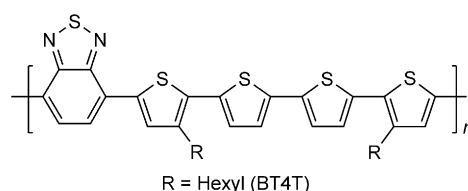
PCPDTBT

Figure 24. Structure of PCPDTBT.

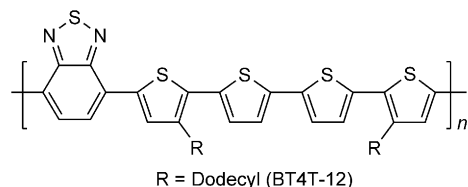
LUMO (P3HT, −2.9 eV; PCPDTBT, −3.55 eV; PCBM, −4.3 eV) and HOMO cascade (P3HT, −5.1 eV; PCPDTBT, −5.3 eV; PCBM, −6.0 eV) arising from the three components allow facile charge separation between P3HT and PCBM, PCPDTBT and PCBM, and between P3HT and PCPDTBT.^[43] The IPCE spectrum confirmed the PCPDTBT contribution to the photocurrent. Integrative mode of time-of-flight (TOF) measurements suggested that P3HT was the major hole transporter and that PCBM was the exclusive electron transporter. V_{oc} , J_{sc} , and the efficiency of the ternary cells increased with increasing PCPDTBT content, up to 20 wt%, although FF did not share this trend.

Recently, Machui et al. pointed out the possibility to obtain important insights into morphological behavior in the P3HT/PCPDTBT/PCBM system through wide-angle X-ray scattering (GiWAXS), differential scanning calorimetric measurements (DSC), and space-charge limited current (SCLC) transport analysis.^[44] They concluded that: i) an increase in the PCPDTBT amount will decrease the PCBM crystallinity; ii) an effect of the PCPDTBT amount can be found on the electron-only device, whereas there is no influence on the hole-only device; and iii) lower J_{sc} and FF were attributed to the reduced PCBM crystallinity.

Addition of a series of BT4T polymers (Figure 25) to the P3HT/PCBM blend broadened the absorption spectrum of the



R = Hexyl (BT4T)



R = Dodecyl (BT4T-12)

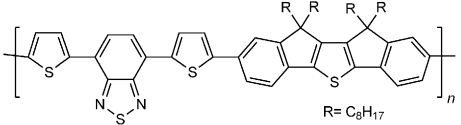
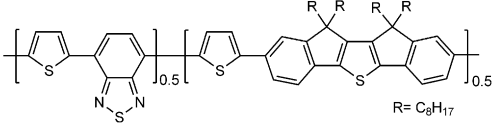
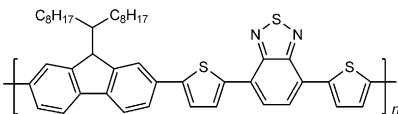
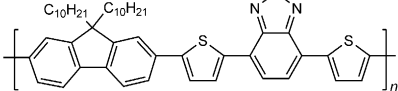
Figure 25. Structures of BT4T series polymers.

active layer and also improved the molecular ordering of P3HT, albeit at the expense of decreased P3HT absorption.^[45] By comparison, crystalline BT4T-12 in the P3HT/BT4T-12 composite showed a decrease in carrier transport at the grain boundaries as well as a reduced FF and device performance. Thus, the P3HT/BT4T/PCBM ternary system operated at 2.52% efficiency, and exhibited better V_{oc} , J_{sc} , and FF than the binary system without BT4T.

Ternary systems using two benzothiadiazole-based polymers as sensitizers were reported by separate research groups.^[46,47] The structures of the dyes and their photovoltaic parameters are listed in Table 1. The complementary absorption and miscibility characteristics of PDIDTDTBT and PTDIDTBT resulted in an improved performance of the resulting ternary cell compared to that of the binary cell using a single polymer.^[46] By comparison, the ternary systems formed with PCDTBT, PFDTBT, and PCBM were less efficient than the binary system using a single sensitizer. The authors attributed the degraded performance to similar absorption profiles and the incompatibility of the two dyes.^[47]

The structure of PCPDTBT is shown in Figure 24; Hsu et al. used two new D–A copolymers, P1 and P5 (Figure 26), as additives in a PCPDTBT/PC₇₁BM active layer.^[48] The PCPDTBT/P1/PC₇₁BM ternary system, with a composite ratio of 1:1:4, exhibited a higher efficiency (2.5%) than the 1:2 PCPDTBT/PC₇₁BM binary system (1.4%) or the 1:2 binary composite P1/PC₇₁BM (2.0%). By contrast, the 1:1:4 PCPDTBT/P5/PC₇₁BM ternary system showed a performance (1.9%) inferior to the 1:2 P5/PC₇₁BM binary system (2.2%). The superior performance of the ternary cell of P1 was credited to the better compatibility of P1 with PCPDTBT because the two dyes had the same donor moieties. Additionally, the ternary blend had a broader spectral coverage.

Sharma et al. prepared two alternating copolymers with phenylenevinylene blocks, PB and P3 (Figure 27a), for solar cell applications.^[49] P, PB, and PCBM have compatible energy alignments (Figure 27b), resulting in efficient charge separation in the device. The generated electrons travel through the PCBM layer to the cathode, and the holes migrate through both P3 and PB to the anode. The PCE of the as-cast 1:1:1 P/PB/PCBM ternary cell reached 2.56%, which was higher than that in

Compounds	Weight ratio copolymer/PCBM	J_{sc} [mA cm ⁻²]	V_{oc} [V]	FF	η [%]
 PTDIDTTBT	1:2	5.3	0.70	0.44	1.65
 PDIDTCTBT	1:4	6.2	0.68	0.47	2.00
PTDIDTTBT/PDIDTCTBT	1:1:8	6.4	0.85	0.43	2.40
 PCDTBT/PFDTBT	1:3	8.84	0.82	0.46	3.34
 PCDTBT/PFDTBT	1:3	8.31	0.78	0.43	2.79
PCDTBT/PFDTBT	0.4:0.6:3	9.01	0.76	0.42	2.88

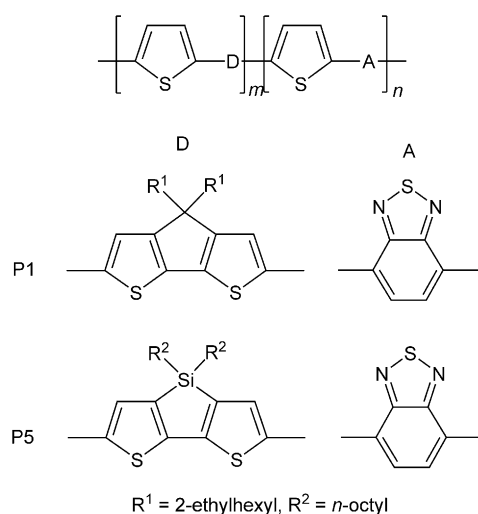


Figure 26. Structures of the P1 and P5.

either the as-cast P3/PCBM (1.15%) or the as-cast PB/PCBM cell (1.57%). After annealing, the PCE of the ternary cell was further increased to 3.48%. Thermal treatment triggered reorganization of P3 and PB in the composite to form more crystalline structures.

You et al. reported BHJ solar cells consisting of two donor polymers (Figure 28) and PCBM.^[50] The polymer pairs, TAZ and DTBT or DTffBT and DTPyT, have similar conjugated skeletons and side chains. Consequently, it is possible to mix the two components in different ratios without phase separation occurring. The ternary cells always performed better than the binary

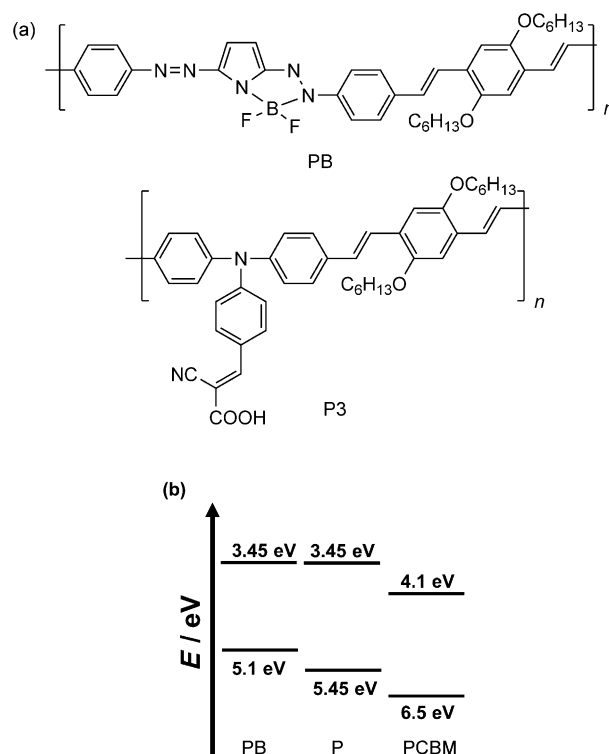


Figure 27. (a) Structures of PB and P3 copolymers, (b) the energy level diagram of the OPV materials.

cells, although the efficiency varied with the dye ratio. For example, i) a ternary device consisting of TAZ/DTBT in a 3:7 weight ratio showed a PCE value of 5.88%, which was better

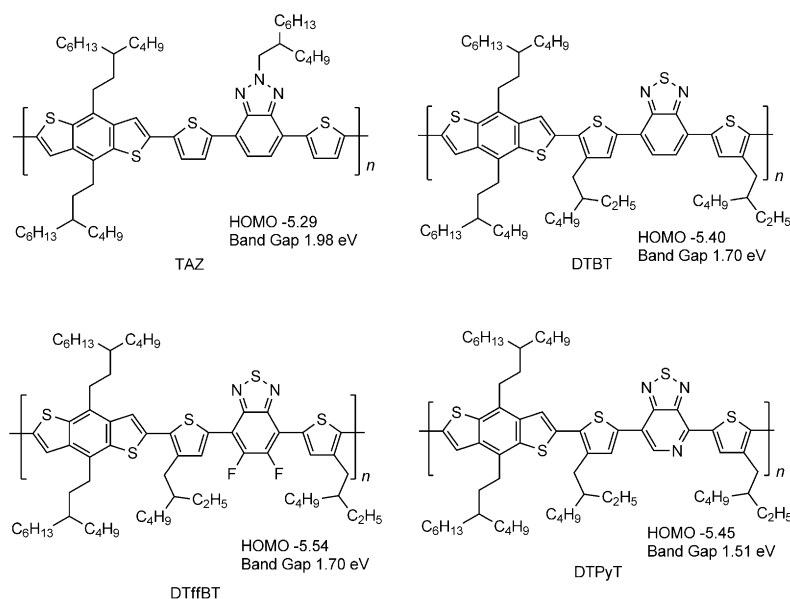


Figure 28. Structures of TAZ, DTBT, DTffBT, and DTPyT polymers.

than that of either TAZ ($\eta = 4.06\%$) or DTBT ($\eta = 4.39\%$) binary devices in a 1:1 ratio with PCBM; and ii) the 1:1 ternary device consisting of DTffBT and DTPyT had a higher PCE (7.02%) than the binary devices based on either DTffBT ($\eta = 6.26\%$) or DTPyT ($\eta = 6.30\%$) in a 1:1 ratio with PCBM. Neither the energy transfer nor the charge transfer between different donor materials played an important role in the cell performance. Instead, the authors proposed that the excitons generated in an individual donor polymer migrate to the respective polymer/PCBM interface, where they dissociate into free electrons and holes. The electrons are then transported through PCBM to the cathode. Ideally, the EQE spectra are approximately the sum of the individual "sub-cells." In their study, You et al. used polymers with complementary absorption characteristics (Figure 28) to investigate the weight ratio effect on OPV device performance.

Thompson et al. also investigated the ternary solar cells containing two P3HT analogues as donor polymers, that is, high-band-gap poly(3-hexylthiophene-co-3-(2-ethylhexyl)thiophene) (P3HT₇₅-co-EHT₂₅) and low-band-gap poly(3-hexylthiophene-thiophene-diketopyrrolopyrrole) (P3HTT-DPP-10%), with PCBM as an acceptor.^[51] They varied the ratio of the three components and found that V_{oc} increased as the amount of P3HT₇₅-co-EHT₂₅ increased. The overall polymer/fullerene ratio of the ternary-blend BHJ solar cells was individually optimized at each polymer/polymer ratio. As a result, the ternary-blend BHJ solar cells showed power conversion efficiencies up to 5.51%, exceeding those of the corresponding binary blends (3.16 and 5.07%). This concept may be applied to multiple donor systems. The authors indicated that a ternary system that used one donor and two acceptors (vide infra) could be also an example cell.^[52]

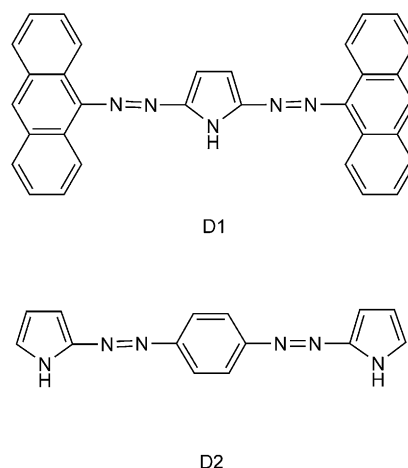


Figure 29. Structures of D1 and D2.

ternary cell was fabricated to take advantage of the complementary absorption bands of the two dyes and the favorable energy levels among D1, D2, and PCBM. Device efficiency reached 3.61% after thermal annealing. Photoluminescence (PL)-quenching studies suggest that the photoinduced charge-transfer effect is faster in ternary systems than it is in binary systems.

Roncali et al. developed the BODIPY compounds **1** and **2** shown in Figure 30 with complementary absorption bands for the use in ternary OPV devices.^[54] The IPCE spectra of the ternary cell based on **1**/2/PCBM in a 1:1:2 ratio showed the contribution of both dyes to the photocurrent (Figure 31). The device had the following performance parameters: $J_{sc} = 4.70 \text{ mA cm}^{-2}$, $V_{oc} = 0.866 \text{ V}$, $FF = 0.42$, and $\eta = 1.70\%$. Both J_{sc} and efficiency were improved in comparison to those of binary cells based on **1**/PCBM ($J_{sc} = 4.43 \text{ mA cm}^{-2}$, $\eta = 1.17\%$) or **2**/PCBM ($J_{sc} = 4.14 \text{ mA cm}^{-2}$, $\eta = 1.34\%$).^[55]

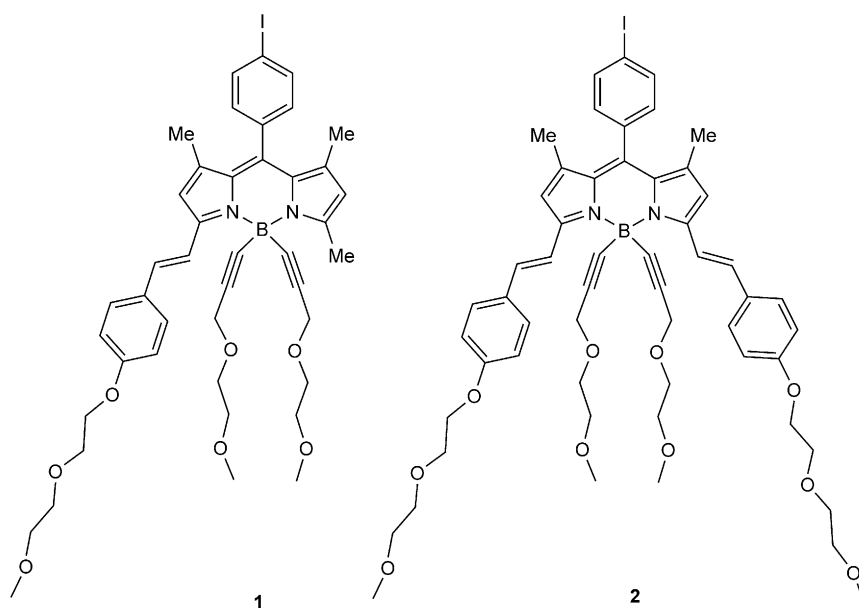


Figure 30. Structures of the BODIPY dyes 1 and 2.

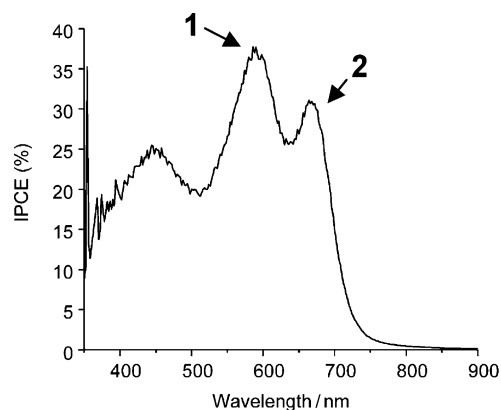


Figure 31. IPCE spectra of the BHJ cell based on 1/2/PCBM in a 1:1:2 weight ratio. Reprinted with permission from Ref. [54]. Copyright 2009, The Royal Society of Chemistry.

3.4. Polymer/PCBM/fullerene derivative-based ternary solar cells

In addition to using two donors and one acceptor (normally PCBM or PC₇₁BM) as the active layer to broaden the device's absorption spectrum and increase the photocurrent, ternary devices using one donor and two acceptors as the active layer have been assembled to increase J_{sc} and V_{oc} . Chen et al. reported the fabrication of ternary systems based on P3HT, PCBM, and a surfactant based on C₆₀-derivatives tethered with a thiophene-containing segment (PCBTTE, PCBBTE, or PCBTTE; Figure 32).^[56] The PCBTTE compound was the most effective additive among these because of its compatibility with P3HT, as determined from surface energy analysis and DSC. A ternary cell based on a 1:0.8 mix of P3HT/PCBM blended with 5% PCBTTE operated at 4.37% efficiency. This was higher than the efficiency (3.85%) of the pristine binary system. The added

PCBTTE was found to improve the ordering of P3HT polymer chains, which proved beneficial for light harvesting and charge transport. Moreover, the introduction of the PCBTTE additive reduced the aggregation of PCBM that occurred during the annealing process, which resulted in an improved thermal stability of the cell, as evidenced by the TEM image (Figure 32).^[56]

Thompson et al. reported a ternary system using P3HT as the donor and two functional fullerenes, PCBM and indene-C₆₀ bis-adduct (ICBA), as the acceptors. The chemical structures and energy levels of PCBM and ICBA are shown in Figure 33.^[52] Photovoltaic properties were investigated for various PCBM and ICBA compositions. The results

indicate that V_{oc} for the ternary BHJ solar cells could be tuned between the limiting V_{oc} values of the corresponding binary solar cells without significant perturbation of J_{sc} or FF . Although the efficiency of the ternary systems did not surpass that of the binary system, this study demonstrated that the photovoltaic parameters of ternary blends are not necessarily constrained by the same factors or constrained by the same limitations as those in binary blends.

Chan et al. developed a C₆₀-containing block copolymer (C₆₀-BCP) as the additive in P3HT/C₆₀ solar cells (Figure 34).^[57] The ternary system based on P3HT/C₆₀ with a 1:0.5 weight ratio and 20 wt% C₆₀-BCP exhibited a 2.56% cell efficiency, a fivefold increase over that of the 1:0.5 ratio P3HT/C₆₀ (0.48%). Additionally, the C₆₀-BCP facilitated the formation of a self-organized nanostructured P3HT domain and reduced interfacial tensions between P3HT and C₆₀, thus increasing the compatibility within the active layer. Because of the poor solubility of C₆₀ in common organic solvents, polymer/C₆₀ blends generally require difficult post-treatments. Use of C₆₀-BCP as an additive to encourage self-organization and active-layer compatibility greatly increases the utility and cost-effectiveness of C₆₀ and has the potential for application in other ternary systems.

4. Polymer/Quantum Dot or Metal/Fullerene Derivative-Based Ternary Solar Cells

Quantum dots (QDs) are promising materials for OPVs because of the possibility of band gap manipulation through size variation of an individual crystal; NIR band gaps are now viable.^[58–60] Hybrid solar cells using inorganic semiconducting nanoparticles, such as TiO₂, ZnO, CuInS₂, PbSe, CdSe and CdTe, as sensitizers have been investigated, and the use of QDs as an additive in binary solar cells was briefly discussed.^[60]

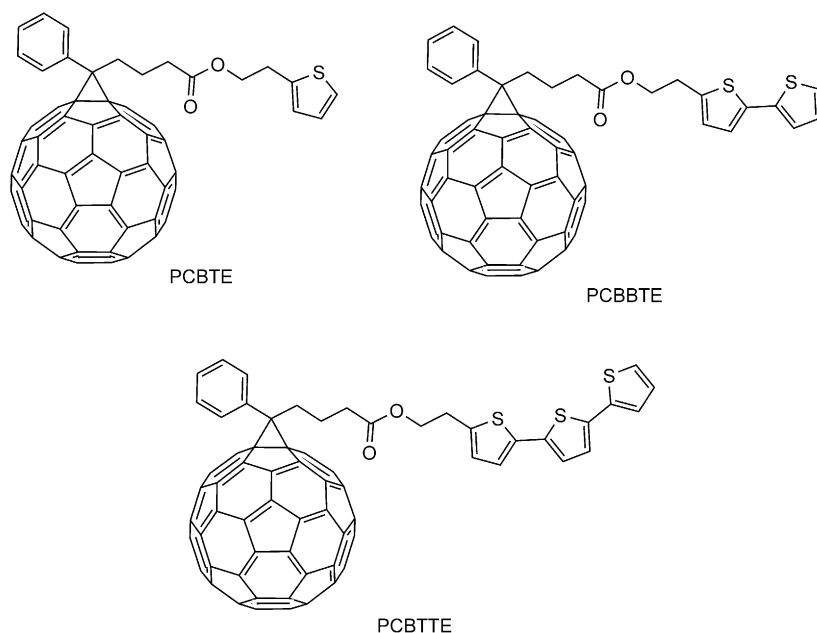


Figure 32. Structures of the C₆₀-derivate compounds PCBTE, PCBBTE, and PCBTTE.

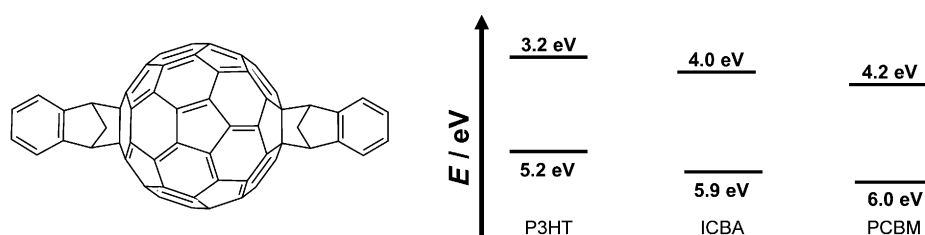


Figure 33. Chemical structure (left) and the relative energy levels of P3HT, ICBA and PCBM (right).

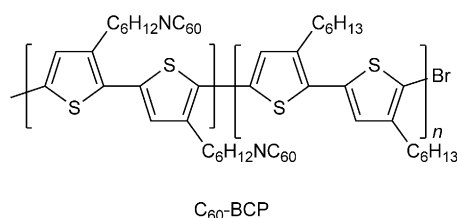


Figure 34. Structure of the C₆₀-BCP compound.

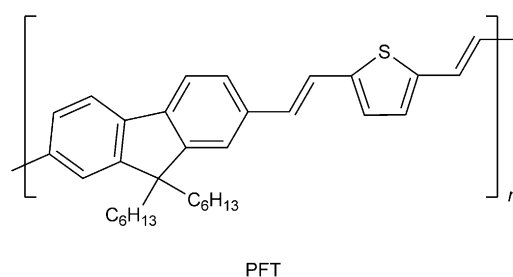


Figure 35. Structure of the PFT polymer.

Doping polymers with nanoparticles enables further tuning of the optical and electronic properties of OPVs. PbS QDs^[61,62] and CdSe QDs^[63,64] are the most common additives for solar cell applications. Nogueira et al. reported a ternary system based on PFT (a PPV-type polymer; Figure 35), PCBM, and CdSe nanoparticles coated with a trioctylphosphine oxide film.^[63] Of the various CdSe/PCBM ratios and differently sized nanoparticles studied, the best performing ternary system, with $\eta = 0.76\%$, $J_{sc} = 4.5 \text{ mA cm}^{-2}$, $V_{oc} = 0.57 \text{ V}$, and $FF = 0.30$, consisted of 20 wt% PFT/40 wt% PCBM/40 wt% CdSe (diameter 4.0 nm); the cell performance surpassed that of the PFT/PCBM binary cell ($\eta = 0.48\%$; $J_{sc} = 3.5 \text{ mA cm}^{-2}$; $V_{oc} = 0.48 \text{ V}$;

$FF = 0.28$). Changes in the PFT/PCBM film morphology after incorporation of CdSe nanoparticles resulted in a significant improvement of the photocurrent and harvesting efficiency of the device. Light absorption by the nanoparticle aggregates was suggested to contribute to device efficiency.

An inverted-structure OPV, FTO/TiO₂/P3HT:PCBM:CdSe (10:10:1)/PEDOT:PSS/Ag, was reported to produce a cell efficiency of 3.05%, surpassing that of the binary system (2.06%).^[64] The cell exhibited a high stability, and 70% of its initial high efficiency was retained after 21 days of exposure to air.

To overcome problems with nanoparticle aggregation, Khan et al. reported the in situ synthesis of cadmium telluride (CdTe) nanoparticles in P3HT.^[65] The authors suggested that dipole-dipole interactions were the dominant process in the formation of a charge-transfer complex between the P3HT donor and the CdTe acceptor. In addition to the broadened absorption, the blend morphology as

well as energy cascade of the HOMO and LUMO energy levels (Figure 36) resulted in an increased J_{sc} compared to the binary system. V_{oc} (0.80 V) was also improved significantly compared to the binary system (0.58 V) because of an increase in the energy-level offset between the donor and acceptor.

Gold nanoparticles strongly interact with incident light because of surface plasma resonance effects, and light scattering increases the optical path length. Chin et al. reported a BHJ device incorporating gold nanoparticles of varying quantity.^[66] Improvements in PCE and J_{sc} were observed for small amounts of the nanoparticle dopant, and up to 2.17% cell efficiency

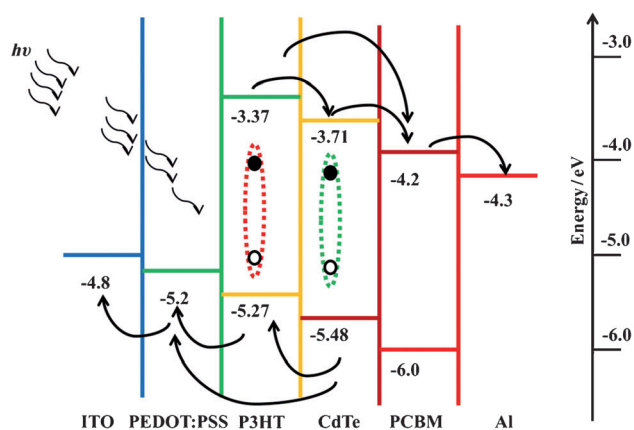


Figure 36. Illustration of the energy diagram for the CdTe-nanoparticle device. Reprinted with permission from Ref. [65]. Copyright 2011, American Institute of Physics.

was achieved for an optimal concentration of gold nanoparticles. This value is significantly higher than that of an OPV without gold nanoparticles (1.43 %).

Heeger et al. added gold nanoparticles with an approximate diameter of 70 nm to the active layer of BHJ cells.^[67] The device performance of up to 6% was achieved using an optimized blend ratio of 5 wt% gold nanoparticles. Light scattering was more important for PCE enhancement than improvements in light harvesting because of the narrow-band plasma resonance of the device. The device also exhibited improved charge transport characteristics.

Lee et al. reported the fabrication of BHJ solar cells consisting of ITO/PEDOT/P3HT:PCBB:Ag nanoparticles/Al (PCBB = [6,6]-

phenyl C₆₁-butyric acid butyl ester, Figure 37), in which the silver nanoparticles were generated in situ in the P3HT/PCBB active layer.^[68] Following incorporation of silver nanoparticles, J_{sc} increased from 9.54 to 10.84 mA cm⁻² and FF increased from 0.59 to 0.62. The authors suggested that the improved efficiency of the silver-containing cell compared to that of the pristine cell (4.03 vs. 3.43%) resulted from more a balanced hole and electron mobility and improvements in charge transport.

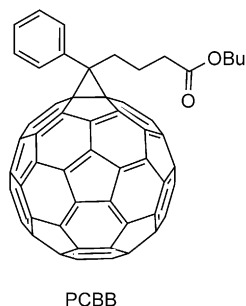


Figure 37. Structure of the C₆₀-derivate compound PCBB.

5. Conclusions

This Review presents a summary of the recent progress in ternary organic solar cells, including organic material/organic material/functional fullerene, organic material/functional fullerene I/functional fullerene II, and organic material/quantum dot or metal/functional fullerene systems. Compared to binary OPV devices, the addition of a third component may increase the short-circuit current through enhanced light harvesting, and/or can increase the open-circuit voltage through enhanced carrier

mobility and modification of HOMO/LUMO energy levels. Careful design of the materials is required to achieve optimal panchromatic absorption, to provide a suitable energy-level offset between the various components, to provide balanced electron and hole mobility, and to achieve good light-harvesting efficiency. Further development of OPV cell functional materials and relevant physical studies are required before ternary devices are seen as viable commercial products.

Acknowledgements

We would like to acknowledge the Institute of Chemistry, Academia Sinica, and National Science Council, Taiwan for financial support.

Keywords: absorption • carrier mobility • charge transfer • energy level • solar cells

- [1] G. Dennler, M. C. Scharber, C. J. Brabec, *Adv. Mater.* **2009**, *21*, 1323–1338.
- [2] J. Peet, M. L. Senatore, A. J. Heeger, G. C. Bazan, *Adv. Mater.* **2009**, *21*, 1521–1527.
- [3] H. Zhou, L. Yang, W. You, *Macromolecules* **2012**, *45*, 607–632.
- [4] B. Walker, C. Kim, T. Q. Nguyen, *Chem. Mater.* **2011**, *23*, 470–482.
- [5] Y. J. Cheng, S. H. Yang, C. S. Hsu, *Chem. Rev.* **2009**, *109*, 5868–5923.
- [6] a) R. F. Service, *Science* **2011**, *332*, 293–293; b) H. Zhou, L. Yang, A. C. Stuart, S. C. Price, S. Liu, W. You, *Angew. Chem.* **2011**, *123*, 3051–3054; *Angew. Chem. Int. Ed.* **2011**, *50*, 2995–2998; c) H. Y. Chen, J. Hou, S. Zhang, Y. Liang, G. Yang, Y. Yang, L. Yu, Y. Wu, G. Li, *Nat. Photonics* **2009**, *3*, 649–653; d) S. C. Price, A. C. Stuart, L. Yang, H. Zhou, W. You, *J. Am. Chem. Soc.* **2011**, *133*, 4625–4631; e) C. M. Amb, S. Chen, K. R. Graham, J. Subbiah, C. E. Small, F. So, J. R. Reynolds, *J. Am. Chem. Soc.* **2011**, *133*, 10062–10065; f) M. S. Su, C. Y. Kuo, M. C. Yuan, U. S. Jeng, C. J. Su, K. H. Wei, *Adv. Mater.* **2011**, *23*, 3315–3319; g) T. Y. Chu, J. Lu, B. Beaupré, Y. Zhang, J. R. Pouliot, S. Wakim, J. Zhou, M. Leclerc, Z. Li, J. Ding, Y. Tao, *J. Am. Chem. Soc.* **2011**, *133*, 4250–4253; h) Y. Liang, Z. Xu, J. Xia, S. T. Tsai, Y. Wu, G. Li, C. Ray, L. Yu, *Adv. Mater.* **2010**, *22*, E135–138; i) Z. He, C. Zhong, X. Huang, W. Y. Wong, H. Wu, L. Chen, S. Su, Y. Cao, *Adv. Mater.* **2011**, *23*, 4636–4643; j) C. E. Small, S. Chen, J. Subbiah, C. M. Amb, S. W. Tsang, T. H. Lai, J. R. Reynolds, F. So, *Nat. Photonics* **2012**, *6*, 115–120.
- [7] J. Chen, Y. Cao, *Acc. Chem. Res.* **2009**, *42*, 1709–1718.
- [8] J. H. Yum, E. Baranoff, S. Wenger, M. K. Nazeeruddin, M. Grätzel, *Energy Environ. Sci.* **2011**, *4*, 842–857.
- [9] a) B. C. Thompson, Y. G. Kim, J. R. Reynolds, *Macromolecules* **2005**, *38*, 5359–5362; b) Y. Kim, S. Cook, S. A. Choulis, J. Nelson, J. R. Durrant, D. D. C. Bradley, *Synth. Met.* **2005**, *152*, 105–108.
- [10] Y. Kim, S. Cook, S. M. Tuladhar, S. A. Choulis, J. Nelson, J. R. Durrant, D. D. C. Bradley, M. Giles, I. McCulloch, C. S. Ha, M. Ree, *Nat. Mater.* **2006**, *5*, 197–203.
- [11] J. Y. Kim, S. H. Kim, H. H. Lee, K. Lee, W. Ma, X. Gong, A. J. Heeger, *Adv. Mater.* **2006**, *18*, 572–576.
- [12] G. P. Smestad, F. C. Krebs, C. M. Lampert, C. G. Granqvist, K. L. Chopra, X. Mathew, H. Takakura, *Sol. Energy Mater. Sol. Cells* **2008**, *92*, 371–373.
- [13] S. Honda, T. Nogami, H. Ohkita, H. Benten, S. Ito, *ACS Appl. Mater. Interfaces* **2009**, *1*, 804–810.
- [14] S. Honda, S. Yokoyama, H. Ohkita, H. Benten, S. Ito, *J. Phys. Chem. C* **2011**, *115*, 11306–11316.
- [15] S. Honda, H. Ohkita, H. Benten, S. Ito, *Chem. Commun.* **2010**, *46*, 6596–6598.
- [16] a) A. Loudet, K. Burgess, *Chem. Rev.* **2007**, *107*, 4891–4932; b) R. Ziessel, G. Ulrich, A. Harriman, *New J. Chem.* **2007**, *31*, 496–501; c) J. Roncali, *Acc. Chem. Res.* **2009**, *42*, 1719–1730.
- [17] Y. Kubo, Z. Watanabe, R. Nishiyabu, R. Hata, A. Murakami, T. Shoda, H. Ota, *Org. Lett.* **2011**, *13*, 4574–4577.

- [18] T. Hasobe, H. Imahori, P. V. Kamat, T. K. Ahn, S. K. Kim, D. Kim, A. Fujimoto, T. Hirakawa, S. Fukuzumi, *J. Am. Chem. Soc.* **2005**, *127*, 1216–1228.
- [19] T. Hasobe, A. S. D. Sandanayaka, T. Wada, Y. Araki, *Chem. Commun.* **2008**, 3372–3374.
- [20] W. J. Belcher, K. I. Wagner, P. C. Dastoor, *Sol. Energy Mater. Sol. Cells* **2007**, *91*, 447–452.
- [21] N. Cooling, K. B. Burke, X. Zhou, S. J. Lind, K. C. Gordon, T. W. Jones, P. C. Dastoor, W. J. Belcher, *Sol. Energy Mater. Sol. Cells* **2011**, *95*, 1767–1774.
- [22] Z. X. Xu, V. A. L. Roy, K. H. Low, C. M. Che, *Chem. Commun.* **2011**, *47*, 9654–9656.
- [23] T. Hori, T. Masuda, N. Fukuoka, T. Hayashi, Y. Miyake, T. Kamikado, H. Yoshida, A. Fujii, Y. Shimizu, M. Ozaki, *Org. Electron.* **2012**, *13*, 335–340.
- [24] J. H. Huang, M. Velusamy, K. C. Ho, J. T. Lin, C. W. Chu, *J. Mater. Chem.* **2010**, *20*, 2820–2825.
- [25] a) B. Walker, A. B. Tamayo, X. D. Dang, P. Zalar, J. H. Seo, A. Garcia, M. Tantiwiwat, T. Q. Nguyen, *Adv. Funct. Mater.* **2009**, *19*, 3063–3069; b) P. Sonar, G. M. Ng, T. T. Lin, A. Dodabalapur, Z. K. Chen, *J. Mater. Chem.* **2010**, *20*, 3626–3636.
- [26] B. P. Karsten, J. C. Bijleveld, R. A. J. Janssen, *Macromol. Rapid Commun.* **2010**, *31*, 1554–1559.
- [27] S. Qu, W. Wu, J. Hua, C. Kong, Y. Long, H. Tian, *J. Phys. Chem. C* **2010**, *114*, 1343–1349.
- [28] J. Peet, A. B. Tamayo, X. D. Dang, J. H. Seo, T. Q. Nguyen, *Appl. Phys. Lett.* **2008**, *93*, 163306.
- [29] J. Lee, M. H. Yun, J. Kim, J. Y. Kim, C. Yang, *Macromol. Rapid Commun.* **2012**, *33*, 140–145.
- [30] G. D. Sharma, S. P. Singh, M. S. Roy, J. A. Mikroyannidis, *Org. Electron.* **2012**, *13*, 1756–1762.
- [31] P. Suresh, P. Balraju, G. D. Sharma, J. A. Mikroyannidis, M. M. Stylianakis, *ACS Appl. Mater. Interfaces* **2009**, *1*, 1370–1374.
- [32] J. A. Mikroyannidis, P. Suresh, G. D. Sharma, *Org. Electron.* **2010**, *11*, 311–321.
- [33] S. S. Sharma, G. D. Sharma, J. A. Mikroyannidis, *Sol. Energy Mater. Sol. Cells* **2011**, *95*, 1219–1223.
- [34] Y. A. M. Ismail, T. Soga, T. Jimbo, *Sol. Energy Mater. Sol. Cells* **2010**, *94*, 1406–1411.
- [35] J. W. Choi, C. Kulshreshtha, G. P. Kennedy, J. H. Kwon, S. H. Jung, M. Chae, *Sol. Energy Mater. Sol. Cells* **2011**, *95*, 2069–2076.
- [36] Q. L. Song, F. Y. Li, H. Yang, H. R. Wu, X. Z. Wang, W. Zhou, J. M. Zhao, X. M. Ding, C. H. Huang, X. Y. Hou, *Chem. Phys. Lett.* **2005**, *416*, 42–46.
- [37] Y. Hayashi, H. Sakuragi, T. Soga, I. Alexandrou, G. A. J. Amaratunga, *Colloids Surf. A* **2008**, *313*–314, 422–425.
- [38] M. C. Chen, D. J. Liaw, Y. C. Huang, H. Y. Wu, Y. Tai, *Sol. Energy Mater. Sol. Cells* **2011**, *95*, 2621–2627.
- [39] G. Adam, A. Pivrikas, A. M. Ramil, S. Tadesse, T. Yohannes, N. S. Sariciftci, D. A. M. Egbe, *J. Mater. Chem.* **2011**, *21*, 2594–2600.
- [40] M. C. Scharber, D. Mühlbacher, M. Koppe, P. Denk, C. Waldauf, A. J. Heeger, C. J. Brabec, *Adv. Mater.* **2006**, *18*, 789–894.
- [41] J. Y. Kim, K. Lee, N. E. Coates, D. Moses, T. Q. Nguyen, M. Dante, A. J. Heeger, *Science* **2007**, *317*, 222–225.
- [42] H. Kim, M. Shin, Y. Kim, *J. Phys. Chem. C* **2009**, *113*, 1620–1623.
- [43] M. Koppe, H. J. Egelhaaf, G. Dennler, M. C. Scharber, C. J. Brabec, P. Schilinsky, C. N. Hoth, *Adv. Funct. Mater.* **2010**, *20*, 338–346.
- [44] F. Machui, S. Rathgeber, N. Li, T. Ameri, C. J. Brabec, *J. Mater. Chem.* **2012**, *22*, 15570–15577.
- [45] E. Lim, S. Lee, K. K. Lee, *Chem. Commun.* **2011**, *47*, 914–916.
- [46] C. H. Chen, Y. J. Cheng, M. Dubosc, C. H. Hsieh, C. C. Chu, C. S. Hsu, *Chem. Asian J.* **2010**, *5*, 2483–2492.
- [47] S. J. Park, J. M. Cho, W. B. Byun, J. C. Le, W. S. Shin, I. N. Kang, S. J. Moon, S. K. Lee, *J. Polym. Sci. Part A* **2011**, *49*, 4416–4424.
- [48] C. H. Chen, C. H. Hsieh, M. Dubosc, Y. J. Cheng, C. S. Hsu, *Macromolecules* **2010**, *43*, 697–708.
- [49] J. A. Mikroyannidis, D. V. Tsagkournos, P. Balraju, G. D. Sharma, *J. Power Sources* **2011**, *196*, 2364–2372.
- [50] L. Yang, H. Zhou, S. C. Price, W. You, *J. Am. Chem. Soc.* **2012**, *134*, 5432–5435.
- [51] P. P. Khlyabich, B. Burkhart, B. C. Thompson, *J. Am. Chem. Soc.* **2012**, *134*, 9074–9077.
- [52] P. P. Khlyabich, B. Burkhart, B. C. Thompson, *J. Am. Chem. Soc.* **2011**, *133*, 14534–14537.
- [53] J. A. Mikroyannidis, D. V. Tsagkournos, S. S. Sharma, A. Kumar, Y. K. Vijay, G. D. Sharma, *Sol. Energy Mater. Sol. Cells* **2010**, *94*, 2318–2327.
- [54] T. Rousseau, A. Cravino, T. Bura, G. Ulrich, R. Ziessel, J. Roncali, *J. Mater. Chem.* **2009**, *19*, 2298–2300.
- [55] T. Rousseau, A. Cravino, T. Bura, G. Ulrich, R. Ziessel, J. Roncali, *Chem. Commun.* **2009**, 1673–1675.
- [56] Y. C. Lai, T. Higashihara, J. C. Hsu, M. Ueda, W. C. Chen, *Sol. Energy Mater. Sol. Cells* **2012**, *97*, 164–170.
- [57] S. H. Chan, C. S. Lai, H. L. Chen, C. Ting, C. P. Chen, *Macromolecules* **2011**, *44*, 8886–8891.
- [58] A. Tang, S. Qu, F. Teng, Y. Hou, Y. Wang, Z. Wang, *J. Nanosci. Nanotechnol.* **2011**, *11*, 9384–9394.
- [59] J. Tang, E. H. Sargent, *Adv. Mater.* **2011**, *23*, 12–29.
- [60] R. Debnath, O. Bakr, E. H. Sargent, *Energy Environ. Sci.* **2011**, *4*, 4870–4881.
- [61] T. Rauch, M. Böberl, S. F. Tedde, J. Fürst, M. V. Kovalenko, G. Hesser, U. Lemmer, W. Heiss, O. Hayden, *Nat. Photonics* **2009**, *3*, 332–336.
- [62] G. Itskos, A. Othonos, T. Rauch, S. F. Tedde, O. Hayden, M. V. Kovalenko, W. Heiss, S. A. Choulis, *Adv. Energy Mater.* **2011**, *1*, 802–812.
- [63] J. N. de Freitas, I. R. Grova, L. C. Akcelrud, E. Arici, N. S. Sariciftci, A. F. Nogueira, *J. Mater. Chem.* **2010**, *20*, 4845–4853.
- [64] H. Fu, M. Choi, W. Luan, Y. S. Kim, S. T. Tu, *Solid-State Electron.* **2012**, *69*, 50–54.
- [65] M. Taukeer Khan, A. Kaur, S. K. Dhawan, S. Chand, *J. Appl. Phys.* **2011**, *110*, 044509.
- [66] M. Park, B. D. Chin, J. W. Yu, M. S. Chun, S. H. Han, *J. Ind. Eng. Chem.* **2008**, *14*, 382–386.
- [67] D. H. Wang, D. Y. Kim, K. W. Choi, J. H. Seo, S. H. Im, J. H. Park, O. O. Park, A. J. Heeger, *Angew. Chem.* **2011**, *123*, 5633–5637; *Angew. Chem. Int. Ed.* **2011**, *50*, 5519–5523.
- [68] K. B. V. Naidu, J. S. Park, S. C. Kim, S. M. Park, E. J. Lee, K. J. Yoon, S. J. Lee, J. W. Lee, Y. S. Gal, S. H. Jin, *Sol. Energy Mater. Sol. Cells* **2008**, *92*, 397–401.

Received: August 17, 2012

Revised: October 17, 2012

Published online on January 3, 2013